

Journal of Mechanics of Materials and Structures

ANALYSIS OF PEDESTRIAN-INDUCED LATERAL VIBRATION OF A
FOOTBRIDGE THAT CONSIDERS FEEDBACK ADJUSTMENT AND
TIME DELAY

Jia Buyu, Chen Zhou, Yu Xiaolin and Yan Quansheng

Volume 12, No. 5

December 2017



ANALYSIS OF PEDESTRIAN-INDUCED LATERAL VIBRATION OF A FOOTBRIDGE THAT CONSIDERS FEEDBACK ADJUSTMENT AND TIME DELAY

JIA BUYU, CHEN ZHOU, YU XIAOLIN AND YAN QUANSHENG

Research on pedestrian-bridge dynamic interaction has intensified in recent years after the occurrence of several footbridge accidents caused by pedestrian-induced vibration. This study focuses on the analysis of pedestrian-induced lateral vibration of footbridges by considering the time delay and feedback adjustment that occur in the interaction between the pedestrians and the footbridge. A detailed nonlinear lateral vibration model is first established. Then, the bifurcation and stability of this model around the critical value of time delay is discussed using a qualitative method. Moreover, response amplitude and the critical number of pedestrians are evaluated using a multiscale method. Analysis of the results shows that the time delay and feedback adjustment play important roles in controlling the lateral vibration of the footbridge.

1. Introduction

Pedestrian load is considerably smaller than vehicle load; consequently, pedestrian-induced vibration of footbridges has not aroused considerable attention until the occurrence of the Millennium Bridge accident in London, which was caused by large lateral vibration. Unlike a running vehicle, a pedestrian creates an alternating motion as they walk with their two legs; this does not only produce a vertical force but also lateral and longitudinal forces. The normal pedestrian walking frequency ranges from 1.6 Hz to 2.4 Hz in the vertical direction, from 0.8 Hz to 1.2 Hz in the lateral direction, and from 0.8 Hz to 1.2 Hz in the longitudinal direction [Živanović et al. 2005]. Meanwhile, the fundamental frequencies of most flexible footbridges are less than 3.0 Hz, which indicates that the walking frequency of pedestrians falls within the range of the fundamental frequency of most footbridges. That is, the walking action of a pedestrian may easily cause resonance on a footbridge. Accidents caused by large vibrations have occurred in recent years. For example, a steel suspension footbridge in the Sichuan Province in China collapsed in 2010 because of a large lateral vibration caused by walking tourists; the accident left over 28 people injured [Qin 2013]. Apart from causing collapse failure, the footbridge vibration frequently leads to discomfort among pedestrians. Pedestrians are highly sensitive to footbridge vibration; therefore, a large footbridge vibration can make pedestrians feel uncomfortable and even cause panic in a crowd. The large lateral vibration of the Millennium Bridge is a famous example [Dallard et al. 2001a]. The Millennium Bridge

This research was supported by the National Natural Science Foundation of China (Nos. 51478193), the China Postdoctoral Science Foundation (Nos. 2016M592490), the Fundamental Research Funds for the Central Universities (Nos. 2015ZM114), and the Open Fund of State Key Laboratory of Bridge Engineering Structural Dynamics (Nos. 201507).

Keywords: footbridge, nonlinear vibration, lateral displacement, time delay, feedback adjustment.

was temporarily closed for 20 months until the vibration was reduced by implementing several temporary solutions. This incident has become a symbol of pedestrian-induced vibration of footbridges.

Since the occurrence of large lateral vibration of the London Millennium Bridge during its inauguration, experts have started to study the involved mechanisms. In recent years, a number of tests and theoretic models have been investigated to explain the large lateral vibration of footbridges.

Prior to the retrofit of the Millennium Bridge, a full scale test was implemented [Dallard et al. 2001a]. The test showed that there exists a critical number of pedestrians needed to trigger a divergence of lateral vibration. The test also showed that the pedestrian-induced lateral force is proportional to the velocity of bridge, which means the action of pedestrians could be treated as negative viscous dampers. Brownjohn et al. [2004a; 2004b] performed a test on pedestrians circumambulating on a bridge in the Singapore Changi Airport. According to the test, pedestrians might slow down or stop moving forward, depending on the state of bridge vibration. The test also showed that the critical number of pedestrians cannot be determined in a repeatable way due to the randomness of pedestrian walking characteristics.

While walking on a lateral vibrating footbridge, pedestrians continually adjust their states to walk comfortably, and the phenomenon of “lock-in” (pedestrians synchronizing their steps with the bridge’s movement) may occur when the walking frequency of pedestrians is close to the bridge’s lateral natural frequency, which further enhances the lateral vibration. Dallard et al. [2001a] defined this kind of mechanism as Synchronous Lateral Excitation (SLE). To explain the large pedestrian-induced lateral vibration, several models have been proposed and classified into linear response models and nonlinear response models [Ingólfsson et al. 2012]. Linear response models can also be regarded as direct resonance models, where the lateral vibrations are caused by direct resonance; namely, the pedestrian walking frequency is in resonance with the natural frequency of one or more lateral vibration modes. Fujino et al. [1993] considered the direct resonance as the source that excites the large pedestrian-induced lateral vibration and used a linear monodimensional damped dynamical system to analyze the lateral vibration of the T-Bridge. The test on the Millennium Bridge [Dallard et al. 2001a] showed that the first lateral frequency of the central span is 0.48 Hz, which does not fall in the range of pedestrian lateral walking frequencies. This means the direct resonance is not able to explain the large vibration of the first lateral mode of the central span of the Millennium Bridge. It is interesting to note that the second lateral frequency of the central span is around 1 Hz, which may lead to a mixed resonant-parametric excitation. However, such higher mode excitation will not be considered here, as the research’s object is the large vibration of the first lateral mode.

For the nonlinear response model, there are several remarkable models. Based on the Dallard model [Dallard et al. 2001a], which is widely used as a stability criterion to estimate the number of pedestrians needed to trigger large lateral vibration, Nakamura [2004] proposed a refined model by multiplying the lateral force with a modulated function. The modulated function represents the self-limiting nature of the pedestrian synchronization: pedestrians will reduce their walking speed, or completely stop, when the bridge’s velocity becomes large. Yuan [2006] proposed an empirical model, in which the dynamic load factor and the probability of synchronization depend on the vibration amplitude. In this model, both of the self-excited effect caused by the synchronized pedestrians and the forced vibration effect caused by the unsynchronized pedestrians are considered, and a nonlinear equation for stability criterion is derived to estimate the critical number of pedestrians. Blekherman [2005] proposed an autoparametric resonance model to explain the large lateral vibration. Based on the model of Blekherman, the large lateral vibration

in the footbridge can be attributed to the existence of an integer ratio between vertical and lateral mode frequencies. For example, there is a 2 : 1 ratio between the third vertical mode frequency (1.89 Hz) and the second lateral mode frequency (0.95 Hz) in central span of the Millennium Bridge, as well as a 2 : 1 ratio between the third vertical mode frequency (2.0 Hz) and the first lateral mode frequency (1.0 Hz) in the T-Bridge. Besides the autoparametric resonance model, there is another parametric resonance nonlinear model proposed by Piccardo and Tubino [2008], which is based on a displacement-dependent nonlinear lateral force model. According to this model, the large lateral vibration in the flexible footbridge can be attributed to the parametric resonance in which the lateral natural frequency is equivalent to half of the pedestrian lateral walking frequency. For example, in the Millennium Bridge, the first lateral frequency (0.48 Hz) is nearly half of the pedestrian lateral walking frequency (1.0 Hz).

As mentioned previously, pedestrians will make a feedback adjustment according to the bridge vibration. During the process of adjustment, there exists a time delay among the pedestrian-bridge interaction. Based on the Nakamura model, Liu and Xie [2013] proved that the time delay has a great influence on the lateral vibration of footbridge. Newland [2004] assumed that pedestrian movement was composed of two parts. The first part is the natural movement of a pedestrian while walking on a stationary pavement; the second part is the movement caused by the bridge vibration, which is proportional to the bridge amplitude with a time delay. However, Newland did not conduct a specific study on the effect of time delay.

The Millennium Bridge is used as the background in this study. A qualitative analytical method and a multiscale method are used to analyze pedestrian-induced lateral vibration of a footbridge by considering the time delay and feedback adjustment. In addition, the effects of time delay and feedback adjustment on the critical number of pedestrians and response amplitude are discussed.

2. Basic nonlinear vibration model

A footbridge is modeled as a beam under the action of pedestrians. A segment with length ds , which is x distance from the beam support, is considered (Figure 1).

The cross sections are assumed to remain normal to the deformed axis. Using the displacement method, the equilibrium equation of lateral motions at the centroid is obtained as [Chopra 1981]

$$(\rho_s A + m_p) \frac{\partial^2 w}{\partial t^2} ds + \mu_2 \frac{\partial w}{\partial t} ds = \frac{\partial}{\partial s} (N \sin \theta - Q \cos \theta) ds + f_i ds, \tag{1}$$

where ρ_s is the density of the footbridge, A is the section area, m_p is the crowd mass per meter along the bridge, $w(x, t)$ is the lateral displacement, μ_2 is the lateral damping coefficient of the footbridge, θ is the

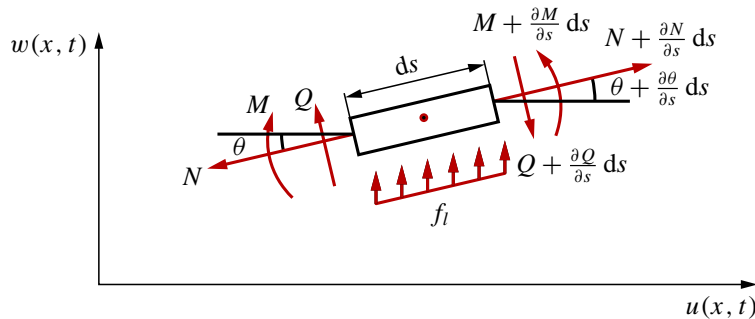


Figure 1. Segment equilibrium.

section angle, $N(x, t)$ is the axial force, $Q(x, t)$ is the shear force, and f_l is the lateral force of pedestrians. Realizing that the pedestrian motion is harmonic and that there exists a time delay (the footbridge vibration does not vary immediately) between the bridge and the pedestrians when the pedestrians-bridge action takes place, the expression of f_l with consideration of a time delay τ can be written as

$$f_l(t - \tau) = \lambda \alpha_l m_p g \cos(\omega_p(t - \tau)), \quad (2)$$

where λ is the pedestrian synchronous coefficient (according to Piccardo and Tubino [2008], the value of λ in the Millennium Bridge is set as $\lambda = 0.3$), g is the acceleration of gravity, ω_p is the pedestrian walking frequency, and α_l is the lateral dynamic loading factor of the first harmonic (the ratio between the lateral dynamic force and the pedestrian weight).

According to the measured data from the literature [Dallard et al. 2001a], it can be found that the pedestrian lateral force is proportional to the lateral velocity of footbridge. Thus, it is assumed that there is a linear relationship between the pedestrian lateral force and the lateral velocity of footbridge, and α_l can be defined as

$$\alpha_l = \alpha_{l1} + \alpha_{l2} \frac{\partial w(x, t - \tau)}{\partial t}, \quad (3)$$

where α_{l1} is the dynamic load coefficient while walking on stationary pavement and α_{l2} is the dynamic load coefficient related to the lateral velocity of footbridge. Subsequently, the pedestrian lateral force can be rewritten as

$$f_l(t - \tau) = \lambda \left[\alpha_{l1} + \alpha_{l2} \frac{\partial w(x, t - \tau)}{\partial t} \right] m_p g \cos(\omega_p(t - \tau)). \quad (4)$$

The fit method is used to approximate the linear relationship between the dynamic load coefficient and the lateral velocity of footbridge (Figure 2). The fitting results show that the values of α_{l1} and α_{l2} in the Millennium Bridge are $\alpha_{l1} = 0.04$ and $\alpha_{l2} = 0.7$.

Assuming that shear force $Q(x, t)$ and moment $M(x, t)$ exhibit the relationship $Q = \partial M / \partial s = \cos \theta (\partial M / \partial x)$, then (1) can be rewritten as

$$(\rho_s A + m_p) \frac{\partial^2 w}{\partial t^2} + \mu_2 \frac{\partial w}{\partial t} = \frac{\partial}{\partial x} \left(N \sin \theta - \frac{\partial M}{\partial x} \cos^2 \theta \right) \cos \theta + f_l(t - \tau). \quad (5)$$

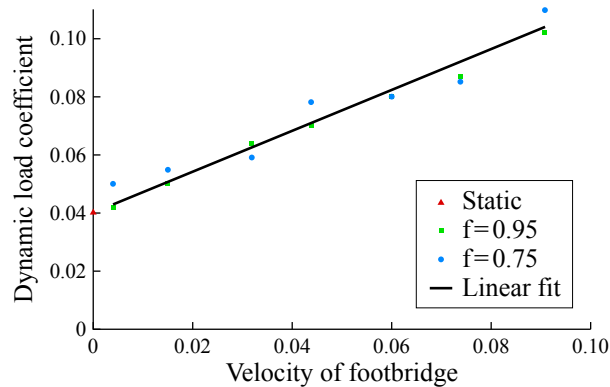


Figure 2. Dynamic load coefficient versus lateral velocity of footbridge.

Through the stress integration on the section, the axial force caused by lateral bend is obtained as

$$N(x, t) = \iint E \varepsilon_N dA = E \iint \frac{\partial \left[\int_0^x \sqrt{1 + (\partial w / \partial x)^2} dx - x \right]}{\partial s} dA, \quad (6)$$

where ε_N is the normal strain caused by lateral bend. $N(x, t)$ is rewritten (based on the first-order Taylor Series expansion of ε_N and $\cos \theta$) as

$$\begin{aligned} N(x, t) &\approx E \iint \frac{\partial \left[\int_0^x \left[1 + \frac{1}{2} (\partial w / \partial x)^2 \right] dx - x \right]}{\partial s} \cos \theta dA \\ &= E \iint \frac{1}{2} \left(\frac{\partial w}{\partial x} \right)^2 \cos \theta dA \approx \frac{1}{2} EA \left(\frac{\partial w}{\partial x} \right)^2. \end{aligned} \quad (7)$$

The moment caused by section rotation is obtained as

$$M(x, t) = EI \frac{\partial \theta}{\partial x} = EI \frac{\partial^2 w}{\partial x^2}. \quad (8)$$

Taking the first-order Taylor series expansion of $\sin \theta$ yields $\sin \theta \approx \theta = \partial w / \partial x$. Accordingly, one has $\cos \theta \approx 1 - (\partial w / \partial x)^2$. Then substituting (7) and (8) into (5), the dynamic equation that contains the only unknowns of the lateral displacement is obtained as

$$\begin{aligned} (\rho_s A + m_p) \frac{\partial^2 w}{\partial t^2} + \mu_2 \frac{\partial w}{\partial t} + EI \frac{\partial^4 w}{\partial x^4} \\ = \frac{3}{2} EA \left(\frac{\partial w}{\partial x} \right)^2 \frac{\partial^2 w}{\partial x^2} + EI \frac{\partial^4 w}{\partial x^4} \left(\frac{\partial w}{\partial x} \right)^2 + 6EI \frac{\partial^3 w}{\partial x^3} \frac{\partial^2 w}{\partial x^2} \frac{\partial w}{\partial x} + 2EI \left(\frac{\partial^2 w}{\partial x^2} \right)^3 + f_l(t - \tau). \end{aligned} \quad (9)$$

When walking on a lateral vibrating footbridge, pedestrians would adjust their strides to walk comfortably, according to the feedback of vibration. The action exerted by the pedestrians on the bridge changes with the bridge vibration. During the early stage of adjustment, the pedestrians' action based on the feedback of vibration may continually enhance the vibration. However, when the lateral vibration amplitude of bridge becomes large enough to make the pedestrians feel uncomfortable, pedestrians will reduce their walking speed or stop walking to lower their actions on the bridge, and then the bridge vibration decreases. These findings suggest that the pedestrians' feedback adjustment is a very complicated process. The mechanism of pedestrians' feedback adjustment involves some uncertain influencing factors, such as pedestrians' psychology, bridge deck typology, human-human interaction, etc. Unfortunately, there is no model or law so far that can precisely describe the pedestrians' feedback adjustment. In this study, a factor ζ is used to comprehensively represent these influencing factors. Then the term $\zeta w(t - \tau)$, which is obtained by multiplying the factor ζ with the lateral displacement of the bridge that allows for the time delay, is introduced to describe the action of feedback adjustment. By adding the term $\zeta w(t - \tau)$ into the (9), we obtain the following:

$$\begin{aligned} (\rho_s A + m_p) \frac{\partial^2 w}{\partial t^2} + \mu_2 \frac{\partial w}{\partial t} + EI \frac{\partial^4 w}{\partial x^4} \\ = \frac{3}{2} EA \left(\frac{\partial w}{\partial x} \right)^2 \frac{\partial^2 w}{\partial x^2} + EI \frac{\partial^4 w}{\partial x^4} \left(\frac{\partial w}{\partial x} \right)^2 + 6EI \frac{\partial^3 w}{\partial x^3} \frac{\partial^2 w}{\partial x^2} \frac{\partial w}{\partial x} + 2EI \left(\frac{\partial^2 w}{\partial x^2} \right)^3 + f_l(t - \tau) + \zeta w(t - \tau). \end{aligned} \quad (10)$$

This study intends to explain the large first lateral vibration of the central span of the Millennium Bridge on the basis of parametric vibration. The second-order factor will not be considered in this study, because the second-order factor corresponds to a direct resonance at second lateral mode (the second lateral frequency of the central span is close to the pedestrian lateral walking frequency). Therefore, the first-order mode $w(x, t) = \psi(x)w_1(t)$ is only considered, where the mode shape function is considered as

$$\phi(x) = \sin(\pi x/l). \quad (11)$$

By using the Galerkin method to execute a discretization, the corresponding modal differential equation is given as

$$\ddot{w}_1(t) + \zeta_1 \dot{w}_1(t) + \omega_1^2 w_1(t) - \zeta_2 \cos(\omega_p(t-\tau)) \dot{w}_1(t-\tau) + \beta w_1^3(t) - h w_1(t-\tau) - F_0 \cos(\omega_p(t-\tau)) = 0, \quad (12)$$

where $\zeta_1 = 2\zeta_0\omega_1$ (ζ_0 is the damping ratio of a footbridge), and

$$\omega_1 = \sqrt{\frac{EI\pi^4}{l^4(\rho_s A + m_p)}}, \quad \zeta_2 = \frac{\lambda\alpha_{l2}m_p g}{\rho_s A + m_p}, \quad \beta = \frac{10EI\pi^6 + 3\pi^4 l^2 EA}{8l^6(\rho_s A + m_p)},$$

$$F_0 = \frac{4\lambda\alpha_{l1}m_p g}{\pi(\rho_s A + m_p)}, \quad \text{and} \quad h = \frac{4\zeta}{\pi(\rho_s A + m_p)}.$$

3. Critical values of time delay

Let $q_1(t) = w_1(t)$ and $q_2(t) = \dot{w}_1(t)$. Equation (12) can be rewritten as

$$\begin{aligned} \dot{q}_1(t) &= q_2(t), \\ \dot{q}_2(t) &= -\zeta_1 q_2(t) + \zeta_2 \cos(\omega_p(t-\tau)) q_2(t-\tau) \\ &\quad - \omega_1^2 q_1(t) - \beta q_1^3(t) + h q_1(t-\tau) + F_0 \cos(\omega_p(t-\tau)). \end{aligned} \quad (13)$$

Let $\bar{\zeta}_2 = \zeta_2 \cos(\omega_p(t-\tau))$. The following characteristic equation that corresponds to (13) can be obtained by adopting a linearization method [Zhen et al. 2013]:

$$\lambda^2 + \zeta_1 \lambda + \omega_1^2 - \bar{\zeta}_2 \lambda e^{-\lambda\tau} - h e^{-\lambda\tau} = 0. \quad (14)$$

Let $\lambda = \kappa + i\nu$ and substitute it into (14). The real part and the imaginary part can be respectively expressed by

$$\kappa^2 - \nu^2 + \zeta_1 \kappa + \omega_1^2 - \bar{\zeta}_2 e^{-\lambda\tau} [\kappa \cos(\nu\tau) + \nu \sin(\nu\tau)] - h e^{-\kappa\tau} \cos(\nu\tau) = 0, \quad (15)$$

$$2\kappa\nu + \zeta_1\nu - \bar{\zeta}_2 e^{-\lambda\tau} [\nu \cos(\nu\tau) - \kappa \sin(\nu\tau)] + h e^{-\kappa\tau} \sin(\nu\tau) = 0. \quad (16)$$

Hopf bifurcation may occur near the origin of (14) when κ changes within a small range around zero; thus, (15) and (16) can be respectively rewritten as

$$-\nu^2 + \omega_1^2 = \bar{\zeta}_2 \nu \sin(\nu\tau) + h \cos(\nu\tau), \quad (17)$$

$$\zeta_1 \nu = \bar{\zeta}_2 \nu \cos(\nu\tau) - h \sin(\nu\tau). \quad (18)$$

Combining (17) with (18) and considering the elimination of time delay τ yields

$$\nu^4 - (2\omega_1^2 + \bar{\zeta}_2^2 - \zeta_1^2)\nu^2 + \omega_1^4 - h^2 = 0. \quad (19)$$

According to (17) and (19), we have

$$v_k = \sqrt{\frac{2\omega_1^2 + \bar{\zeta}_2^2 - \zeta_1^2 \pm \sqrt{4h^2 + (\bar{\zeta}_2^2 - \zeta_1^2)^2 + 4\omega_1^2(\bar{\zeta}_2^2 - \zeta_1^2)}}{2}}, \quad k = 1, 2; \quad (20)$$

$$\tau_{n,k} = \frac{1}{v_{1,2}} \left[\arcsin\left(\frac{\omega_1^2 - v_{1,2}^2}{\sqrt{\bar{\zeta}_2^2 v_{1,2}^2 + h^2}}\right) - \arctan\left(\frac{h}{\bar{\zeta}_2 v_{1,2}}\right) + 2n\pi \right], \quad n = 0, 1, 2, 3, \dots \quad k = 1, 2. \quad (21)$$

When $\tau = \tau_{n,k}$, the complex conjugate roots of (14) may cross the imaginary axis if the following conditions are satisfied:

- (1) a real root of (19) exists, and
- (2) the real part of $d\lambda/d\tau$ is not equal to zero.

The stability and bifurcation of (14) is considered in this study. Note that κ and v in (15) and (16) are functions of τ ; hence, the solutions with the form of $\kappa(\tau) \pm i\nu(\tau)$ are considered. Let $\kappa(\tau_{n,k}) = 0$, $v_k = v_k(\tau_{n,k})$, and $n = 0, 1, 2, 3, \dots$, $k = 1, 2$. Implementing the partial derivative with (15) and (16) yields

$$\begin{aligned} & [\zeta_1 + h\tau \cos(v_k\tau) - \bar{\zeta}_2 \cos(v_k\tau) + \bar{\zeta}_2\tau v_k \sin(v_k\tau)] \frac{d\kappa}{d\tau} \\ & + [-2v_k + h\tau \sin(v_k\tau) - \bar{\zeta}_2 \sin(v_k\tau) - \bar{\zeta}_2\tau v_k \cos(v_k\tau)] \frac{dv_k}{d\tau} \\ & = -hv_k \sin(v_k\tau) + \bar{\zeta}_2 v_k^2 \cos(v_k\tau), \quad k = 1, 2; \quad (22) \end{aligned}$$

$$\begin{aligned} & [2v_k - h\tau \sin(v_k\tau) + \bar{\zeta}_2 \sin(v_k\tau) + \bar{\zeta}_2\tau v_k \cos(v_k\tau)] \frac{d\kappa}{d\tau} \\ & + [\zeta_1 + h\tau \cos(v_k\tau) - \bar{\zeta}_2 \cos(v_k\tau) + \bar{\zeta}_2\tau v_k \sin(v_k\tau)] \frac{dv_k}{d\tau} \\ & = -hv_k \sin(v_k\tau) - \bar{\zeta}_2 v_k^2 \sin(v_k\tau), \quad k = 1, 2. \quad (23) \end{aligned}$$

Combining (22) with (23) yields

$$\frac{d\kappa}{d\tau} = \frac{L_1}{L_2}, \quad (24)$$

where

$$\begin{aligned} L_1 &= -v_k[\bar{\zeta}_2^2 v_k + (2\bar{\zeta}_2 v_k^2 + \zeta_1 h) \sin(v_k\tau) + (2hv_k - \zeta_1 \bar{\zeta}_2 v_k) \cos(v_k\tau)], \\ L_2 &= [\zeta_1 + h\tau \cos(v_k\tau) - \bar{\zeta}_2 \cos(v_k\tau) + \bar{\zeta}_2\tau v_k \sin(v_k\tau)]^2 \\ & + [2v_k - h\tau \sin(v_k\tau) + \bar{\zeta}_2 \sin(v_k\tau) + \bar{\zeta}_2\tau v_k \cos(v_k\tau)]^2, \quad k = 1, 2. \end{aligned}$$

Substituting $\tau = \tau_{n,1}$ and $\tau = \tau_{n,2}$ ($\tau_{n,1} < \tau_{n,2}$) into (24) yields

$$\left. \frac{d\kappa}{d\tau} \right|_{\tau=\tau_{n,1}} < 0, \quad n = 0, 1, 2, 3, \dots; \quad (25)$$

$$\left. \frac{d\kappa}{d\tau} \right|_{\tau=\tau_{n,2}} > 0, \quad n = 0, 1, 2, 3, \dots \quad (26)$$

According to (25) and (26), the stable and unstable regions can be obtained as follows:

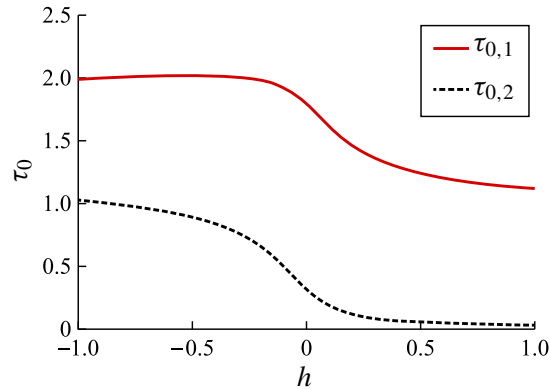


Figure 3. Relationship between the critical value of time delay and the feedback adjustment factor.

- (1) When $d\kappa/d\tau|_{\tau=\tau_{n,1}} < 0$, a pair of eigenvalues cross the imaginary axis, and the real part of the eigenvalues changes from positive to negative. At that moment, the system tends to be stable with an increase in time delay.
- (2) When $d\kappa/d\tau|_{\tau=\tau_{n,2}} > 0$, a pair of eigenvalues cross the imaginary axis, and the real part of the eigenvalues changes from negative to positive. At that moment, the system tends to be unstable with an increase in time delay.

Hence, when h has a certain value, time delay τ will have two corresponding critical values, i.e., $\tau_{n,1}$ and $\tau_{n,2}$, and bifurcations will occur near $\tau_{n,1}$ and $\tau_{n,2}$. Given that $\tau_{n,1} < \tau_{n,2}$, the system is initially stable. When τ arrives at $\tau_{n,2}$, bifurcation occurs, and the system has no real solution. Subsequently, when τ arrives at $\tau_{n,1}$, bifurcation occurs again; at that moment, the system has real solutions. These findings suggest that the lateral vibration of the bridge at first decreases in amplitude as the time delay increases, then it stops altogether when the time delay is in the range $[\tau_{n,1}, \tau_{n,2}]$, and then its amplitude starts increasing again with time delay when the time delay exceeds $\tau_{n,2}$.

Figure 3 shows the relationship between the critical value of time delay and the feedback adjustment factor under $n = 0$ and $\bar{\zeta}_2 = 0.8\zeta_2$. Some conclusions can be derived from Figure 3 as follows:

- (1) When the feedback adjustment factor is fixed at a certain value, the variation of time delay will make the system shift from a balanced state to an unbalanced state and then to another balanced state.
- (2) The critical values of time delay depend on whether the feedback adjustment factor h is positive (pedestrian exerts a feedback adjustment action in an opposite direction to the displacement) or negative (pedestrian exerts a feedback adjustment action in the same direction to the displacement).
- (3) The critical values of time delay vary dramatically around the point of $h = 0$, which denotes that a small feedback adjustment factor will have a relatively large influence on the critical values of time delay.

The aforementioned analysis belongs to the qualitative analysis domain. In the next section, we will adopt a quantitative analysis theory (multiscale method) to discuss the influences of time delay and feedback adjustment on pedestrian-induced lateral vibration of a footbridge.

4. Nonlinear parametric resonance

Back to (12), since the pedestrian modal mass is usually small compared with the structural modal mass, ζ_2 is naturally small, which can be represented by a small parameter ε ; moreover, the terms ζ_1 , β , h and F_0 are also small, and they are assumed small enough to be of the same order as ε . Hence, these parameters mentioned above are rewritten as follows:

$$\zeta_2 = \varepsilon, \quad \zeta_1 = \varepsilon \tilde{\zeta}_1, \quad \beta = \varepsilon \tilde{\beta}, \quad h = \varepsilon \tilde{h}, \quad F_0 = \varepsilon \tilde{F}_0. \quad (27)$$

Letting $r(t) = w_1(t)$ and substituting (27) into (12) yields

$$\ddot{r}(t) + \varepsilon \tilde{\zeta}_1 \dot{r}(t) - \varepsilon \cos(\omega_p(t - \tau)) \dot{r}(t - \tau) \omega_1^2 r(t) + \varepsilon \tilde{\beta} r^3(t) - \varepsilon \tilde{h} r(t - \tau) - \varepsilon \tilde{F}_0 \cos(\omega_p(t - \tau)) = 0. \quad (28)$$

The multiscale method is used to solve (28). The first-order approximation with two time scales is introduced as

$$\begin{aligned} r(t) &= r_0(T_0, T_1) + \varepsilon r_1(T_0, T_1) + O(\varepsilon^2), \quad T_n = \varepsilon^n t, \quad n = 0, 1; \\ r_\tau(t) &= r_{0\tau}(T_0, T_1) + \varepsilon r_{1\tau}(T_0, T_1) + O(\varepsilon^2). \end{aligned} \quad (29)$$

Consider the following differential operators:

$$\begin{aligned} \frac{d}{dT} &= \frac{\partial}{\partial T_0} + \varepsilon \frac{\partial}{\partial T_1} + O(\varepsilon^2) \equiv D_0 + \varepsilon D_1 + O(\varepsilon^2), \\ \frac{d^2}{dT^2} &= D_0^2 + 2\varepsilon D_0 D_1 + O(\varepsilon^2). \end{aligned} \quad (30)$$

Substituting (29) and (30) into (28), and equating the same power of ε yields

$$\varepsilon^0 : D_0^2 r_0 + \omega_1^2 r_0 = 0, \quad (31)$$

$$\begin{aligned} \varepsilon^1 : D_0^2 r_1 + \omega_1^2 r_1 &= -2D_0 D_1 r_0 - \tilde{\zeta}_1 D_0 r_0 + D_0 r_{0\tau} \cos(\omega_p(t - \tau)) \\ &\quad - \tilde{\beta} r_0^3 + \tilde{h} r_{0\tau} + \tilde{F}_0 \cos(\omega_p(t - \tau)). \end{aligned} \quad (32)$$

The solution to (31) is

$$r_0(T_0, T_1) = A(T_1) e^{j\omega_1 T_0} + \bar{A}(T_1) e^{-j\omega_1 T_0}. \quad (33)$$

The time delay term can then be written as

$$r_{0\tau}(T_0, T_1) = A_\tau(T_1) e^{j\omega_1(T_0 - \tau)} + \bar{A}_\tau(T_1) e^{-j\omega_1(T_0 - \tau)}, \quad (34)$$

where $A(T_1)$ and $A_\tau(T_1)$ denote the complex functions with respect to T_1 , which will be determined later; and $\bar{A}(T_1)$ and $\bar{A}_\tau(T_1)$ denote the complex conjugate of $A(T_1)$ and $A_\tau(T_1)$, respectively.

Substituting (33) and (34) into (32) yields

$$\begin{aligned} D_0^2 r_1 + \omega_1^2 r_1 &= -(2D_1 A j\omega_1 + \tilde{\zeta}_1 A j\omega_1) e^{j\omega_1 T_0} + \frac{1}{2} j\omega_1 (A_\tau e^{j(\omega_p + \omega_1)(T_0 - \tau)} - \bar{A}_\tau e^{j(\omega_p - \omega_1)(T_0 - \tau)}) \\ &\quad - \tilde{\beta} (A^3 e^{3j\omega_1 T_0} + 3A^2 \bar{A} e^{j\omega_1 T_0}) + \tilde{h} A_\tau e^{j\omega_1(T_0 - \tau)} + \frac{1}{2} \tilde{F}_0 e^{j(\omega_p T_0 - \omega_p \tau)} + cc, \end{aligned} \quad (35)$$

where cc denotes the complex conjugate of all the preceding terms on the right side. On the basis of (35), parametric vibration will occur when $\omega_p \approx 2\omega_1$, whereas forced vibration will occur when $\omega_p \approx \omega_1$. Parametric vibration and forced vibration cannot occur simultaneously under the action of pedestrian

lateral force when considering the first lateral mode of bridge; thus, only parameter vibration $\omega_p \approx 2\omega_1$ is considered in this section. A detuning parameter σ is added, and the equation is assumed as

$$\omega_p = 2\omega_1 + \varepsilon\sigma. \quad (36)$$

Eliminating the secular terms in (35) yields

$$2D_1Aj\omega_1 + \bar{\zeta}_1Aj\omega_1 + \frac{1}{2}j\omega_1\bar{A}_\tau e^{j\sigma T_1} e^{-j(\omega_1 + \varepsilon\sigma)\tau} - \tilde{h}A_\tau e^{-j\omega_1\tau} + 3\tilde{\beta}A^2\bar{A} = 0. \quad (37)$$

When the time delay is not large and ε is extremely small, \bar{A}_τ and A_τ can be respectively rewritten by using Taylor expansion as follows:

$$\bar{A}_\tau(T_1) = \bar{A}(T_1 - \varepsilon\tau) = \bar{A}(T_1) - \varepsilon\tau\bar{A}'(T_1) + \frac{1}{2}\varepsilon^2\tau^2\bar{A}''(T_1) \approx \bar{A}(T_1), \quad (38)$$

$$A_\tau(T_1) = A(T_1 - \varepsilon\tau) = A(T_1) - \varepsilon\tau A'(T_1) + \frac{1}{2}\varepsilon^2\tau^2 A''(T_1) \approx A(T_1). \quad (39)$$

Then, (37) becomes

$$2D_1Aj\omega_1 + \bar{\zeta}_1Aj\omega_1 + \frac{1}{2}j\omega_1\bar{A}(T_1)e^{j\sigma T_1} e^{-j(\omega_1 + \varepsilon\sigma)\tau} - \tilde{h}A(T_1)e^{-j\omega_1\tau} + 3\tilde{\beta}A^2\bar{A} = 0. \quad (40)$$

For convenience, the complex function $A(T_1)$ is written in polar form as

$$A(T_1) = \frac{1}{2}a_1(T_1)e^{j\phi_1(T_1)}, \quad (41)$$

where $a_1(T_1)$ and $\phi_1(T_1)$ are real functions of T_1 . By substituting (41) into (40) and separating the resulting equation into real and imaginary parts, we obtain the following:

$$D_1a_1 = -\frac{1}{2}\tilde{\zeta}_1a_1 - \frac{1}{4}a_2 \cos \psi \cos((\omega_1 + \varepsilon\sigma)\tau) - \frac{1}{4}a_1 \sin \psi \sin((\omega_1 + \varepsilon\sigma)\tau) - \frac{\tilde{h}a_1}{2\omega_1} \sin(\omega_1\tau), \quad (42)$$

$$D_1\psi = \sigma + \frac{1}{2} \sin \psi \cos((\omega_1 + \varepsilon\sigma)\tau) - \frac{1}{2} \cos \psi \sin((\omega_1 + \varepsilon\sigma)\tau) - \frac{3\tilde{\beta}a_1^2}{4\omega_1} + \frac{\tilde{h}}{\omega_1} \cos(\omega_1\tau), \quad (43)$$

where $\psi = \sigma T_1 - 2\phi_1$. For a steady primary resonance, $D_1a_1 = D_1\psi = 0$, which leads to the following equations with consideration of (27):

$$\frac{1}{2}\tilde{\zeta}_1 + \frac{h}{2\omega_1} \sin(\omega_1\tau) = -\frac{1}{4}\tilde{\zeta}_2 \cos \psi \cos((\omega_1 + \varepsilon\sigma)\tau) - \frac{1}{4}\tilde{\zeta}_2 \sin \psi \sin((\omega_1 + \varepsilon\sigma)\tau), \quad (44)$$

$$\varepsilon\sigma - \frac{3\tilde{\beta}a_1^2}{4\omega_1} + \frac{h}{\omega_1} \cos(\omega_1\tau) = \frac{1}{2}\tilde{\zeta}_2 \cos \psi \sin((\omega_1 + \varepsilon\sigma)\tau) - \frac{1}{2}\tilde{\zeta}_2 \sin \psi \cos((\omega_1 + \varepsilon\sigma)\tau). \quad (45)$$

By squaring both sides of (44) and (45) and adding the resulting equations, the amplitude-frequency equation and the phase-frequency equation can be respectively obtained as

$$\left(\tilde{\zeta}_1 + \frac{h}{\omega_1} \sin(\omega_1\tau)\right)^2 + \left(\varepsilon\sigma - \frac{3\tilde{\beta}a_1^2}{4\omega_1} + \frac{h}{\omega_1} \cos(\omega_1\tau)\right)^2 = \frac{1}{4}\tilde{\zeta}_2^2, \quad (46)$$

$$\tan \psi = \frac{\frac{3\tilde{\beta}a_1^2}{4\omega_1} - \frac{h}{\omega_1} \cos(\omega_1\tau) - \varepsilon\sigma - \left[\tilde{\zeta}_1 + \frac{h}{\omega_1} \cos(\omega_1\tau)\right] \tan((\omega_1 + \varepsilon\sigma)\tau)}{\left[\sigma - \frac{3\tilde{\beta}a_1^2}{4\omega_1} + \frac{h}{\omega_1} \cos(\omega_1\tau)\right] \tan((\omega_1 + \varepsilon\sigma)\tau) - \left[\tilde{\zeta}_1 + \frac{h}{\omega_1} \cos(\omega_1\tau)\right]}. \quad (47)$$

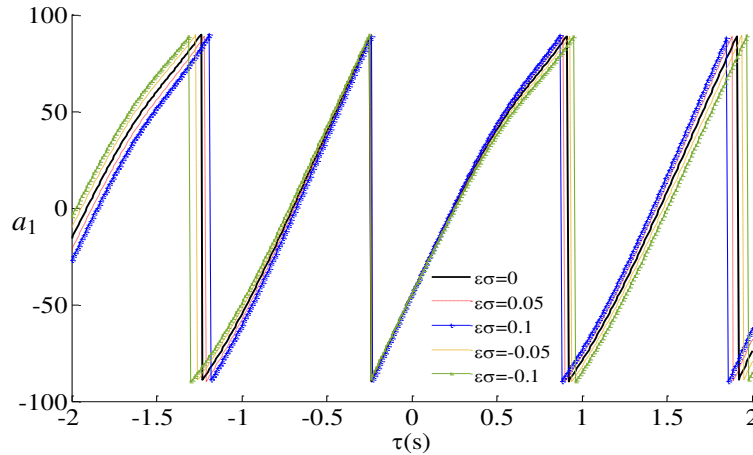


Figure 4. Relationship between phase angle and time delay ($h = 0.05$).

From (46), it can be known that $[\zeta_1 + h/\omega_1 \sin(\omega_1 \tau)]^2 \leq \frac{1}{4} \zeta_2^2$. Note that ζ_2 is probably very small, hence a physical limit range of h can be obtained as $|h| \leq \omega_1 \zeta_1$.

According to (46) and (47), the time delay and feedback adjustment have made a difference in both amplitude and phase.

Figure 4 shows the relationship between phase angle and time delay under different detuning parameters when $h = 0.05$ (rad/s)². As shown in the figure, phase angle changes with time delay, and it has the envelope amplitudes around ± 90 . Moreover, the curves of $\varepsilon\sigma > 0$ and the curves of $\varepsilon\sigma < 0$ are distributed symmetrically on the opposite two sides of the curve of $\varepsilon\sigma = 0$. It is noted that, when time delay is near the region centered around $\tau = -0.23$, the difference between the curve of $\varepsilon\sigma > 0$ and that of $\varepsilon\sigma < 0$ is slight, whereas the difference increases as the time delay becomes farther from the center point.

Solving (46) yields

$$a_1 = \sqrt{\frac{4h}{3\beta} \cos(\omega_1 \tau) + \frac{4\omega_1}{3\beta} \varepsilon\sigma \pm \frac{4\omega_1}{3\beta} \sqrt{\frac{1}{4} \zeta_2^2 - \left(\zeta_1 + \frac{h}{\omega_1} \sin(\omega_1 \tau)\right)^2}}. \quad (48)$$

According to (48), the effect of time delay on response amplitude will be periodic because the time delay is embedded into the triangular functions.

5. Effects of displacement feedback adjustment and time delay on response amplitude

The central span of the Millennium Bridge is used as the background. According to previous works [Dallard et al. 2001b; Piccardo and Tubino 2008], the structural parameters are set as $\omega_1 = 2\pi n_1$ ($n_1 = 0.48$ Hz), $\lambda = 0.3$, $m_s = 2000$ kg/m, $m_{ps} = 70$ kg, $\zeta_0 = 0.007$, and $\alpha_{l2} = 0.7$. It is assumed that 200 pedestrians are walking on the bridge. The response of the Millennium Bridge under parametric resonance (i.e., $\varepsilon\sigma = 0$) is analyzed. Figure 5 shows the effects of the time delay (within a certain period) and feedback adjustment on the response amplitude, in which the feedback adjustment factors are set as $h = \pm 0.05$, $h = \pm 0.1$, and $h = \pm 0.1273$ (the limit range of h is calculated as $[-0.1273, 0.1273]$).

In Figure 5, the solid lines denote stable periodic solutions, whereas the dashed lines denote unstable solutions. Note that no real solution region, which is shown as zero in the figures, exists because the

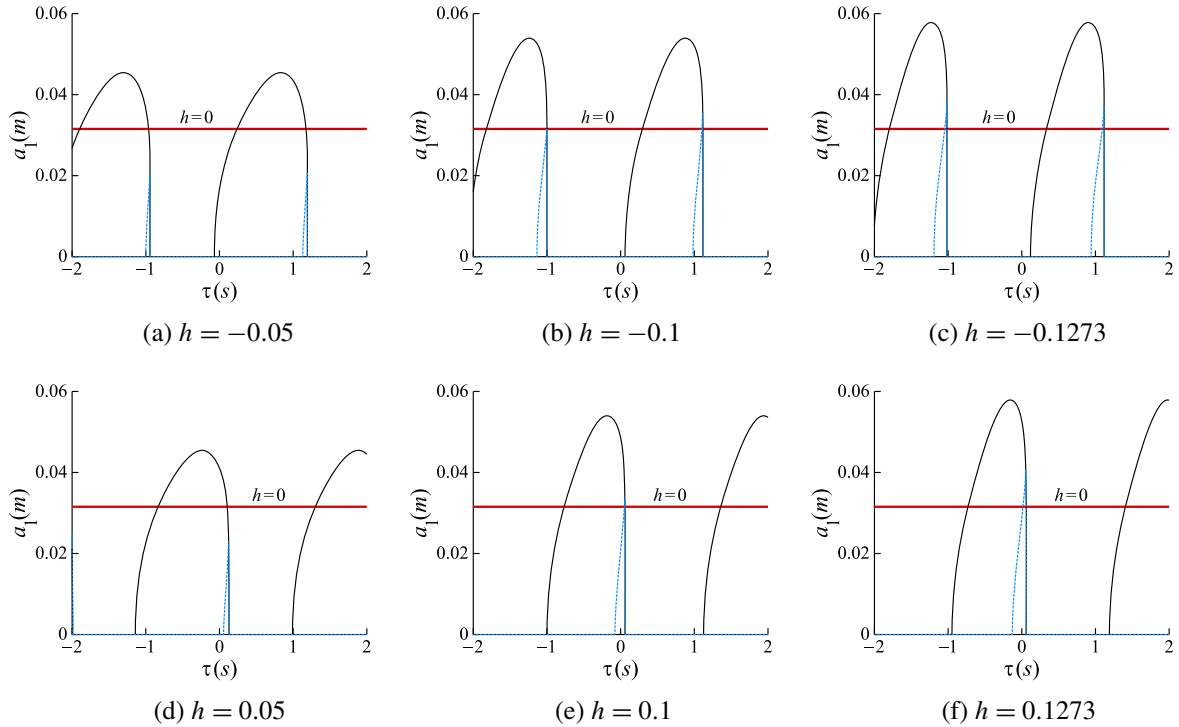


Figure 5. Effects of the time delay and feedback adjustment on response amplitude.

pedestrian-induced vibration of the Millennium Bridge will have a crossing phenomenon caused by the time delay.

The time delay and feedback adjustment significantly affect the response amplitude. As shown in Figure 5, the maximum response amplitude by considering the time delay and feedback adjustment is nearly 0.06, which is almost twice that without feedback adjustment.

A comparison between Figures 5a–5c and Figures 5d–5f shows that the distribution of bridge amplitude with regard to the time delay strongly depends on whether the feedback adjustment factor is positive or negative. Besides, the feedback adjustment factor also affects the maximum response amplitude. The maximum response amplitude increases with the absolute value of feedback adjustment factor.

Meanwhile, the trend of bridge amplitude depends on the time delay. In some time delay regions, the bridge vibration that considers the effect of the feedback adjustment is less than that without feedback adjustment, which means that the feedback adjustment of pedestrians would tend to reduce the bridge vibration, whereas in some other time delay regions, the feedback adjustment of pedestrians would tend to raise the bridge vibration.

6. Effects of the time delay and feedback adjustment on the critical number of pedestrians

Note that amplitude a_1 should be a real number, as given by

$$\frac{4h}{3\beta} \cos(\omega_1 \tau) + \frac{4\omega_1}{3\beta} \varepsilon \sigma \pm \frac{4\omega_1}{3\beta} \sqrt{\frac{1}{4}\zeta_2^2 - \left(\zeta_1 + \frac{h}{\omega_1} \sin(\omega_1 \tau)\right)^2} \geq 0. \quad (49)$$

Subsequently, (49) results in

$$\zeta_2 \leq \zeta_{2 \text{ lim}}, \quad (50)$$

where

$$\zeta_{2 \text{ lim}} = 2\sqrt{\left(\frac{\varepsilon\omega_1\sigma + h \cos(\omega_1\tau)}{\omega_1}\right)^2 + \left(\zeta_1 + \frac{h}{\omega_1} \sin(\omega_1\tau)\right)^2}. \quad (51)$$

According to (51), it can be found that the critical value $\zeta_{2 \text{ lim}}$ of ζ_2 is related to the time delay and feedback adjustment factor.

The pedestrians on the bridge are assumed to be uniformly distributed and the same as the mass distribution of the bridge. This assumption supports the following equation:

$$m_p L = N m_{ps}, \quad (52)$$

where N denotes the number of pedestrians on the bridge, and m_{ps} denotes the mass of a single pedestrian. Combining (50) with (52) yields

$$N \leq \frac{2L\rho_s A \sqrt{\left(\frac{\varepsilon\omega_1\sigma + h \cos(\omega_1\tau)}{\omega_1}\right)^2 + \left(\zeta_1 + \frac{h}{\omega_1} \sin(\omega_1\tau)\right)^2}}{\lambda\alpha_{l2} m_{ps} g - 2m_{ps} \sqrt{\left(\frac{\varepsilon\omega_1\sigma + h \cos(\omega_1\tau)}{\omega_1}\right)^2 + \left(\zeta_1 + \frac{h}{\omega_1} \sin(\omega_1\tau)\right)^2}}. \quad (53)$$

Figures 6a and 6b present the $N - \tau$ curve under different values of h ; Figures 6c and 6d present the $N - h$ curve under different values of τ . Considering the fact that the time delay varies within a certain range under the practical situation, the following analysis will focus on the time delay that is within the range of $[-1, 1]$.

The critical number of pedestrians N depends on different combinations of h and τ . For example, Figure 6a shows that, when $\tau \in [0.37, 0.67]$ and $h < 0$, N decreases with an increase of the absolute value of h . In other words, when the time delay stays within the range of $[0.37, 0.67]$, the action of the negative feedback adjustment may tend to cause large bridge vibration. While for the case of $[0.52, 1]$ and $h < 0$, N increases with τ , denoting that the increase of time delay may tend to reduce the bridge vibration. Meanwhile, the results corresponding to $h > 0$, as shown in Figure 6b, exhibits a trend that is opposite to that of $h < 0$.

Figures 6c and 6d show that, when under the case of $\tau \in [-0.18, 0]$ and $h \in [0, 0.11]$, or the case of $\tau \in [0, 0.18]$ and $h \in [-0.11, 0]$, the corresponding critical number of pedestrians N is consistent with experimental observation (165 ~ 185) on the Millennium Bridge.

It is worth noting that in the case of $h = -0.1273$ and $\tau = 0.52$, or the case of $h = 0.1273$ and $\tau = -0.52$, the critical number of pedestrians N achieves a physical limit of nearly zero. This finding also demonstrates that the limited range of h is about $[-0.1273, 0.1273]$ from another perspective.

7. Amplitude-frequency response curves

Figure 7 shows the amplitude-frequency response curves of the Millennium Bridge under different numbers of pedestrians by assuming that $h = -0.11$ and $\tau = 0.18$.

Some following conclusions can be derived from Figure 7:

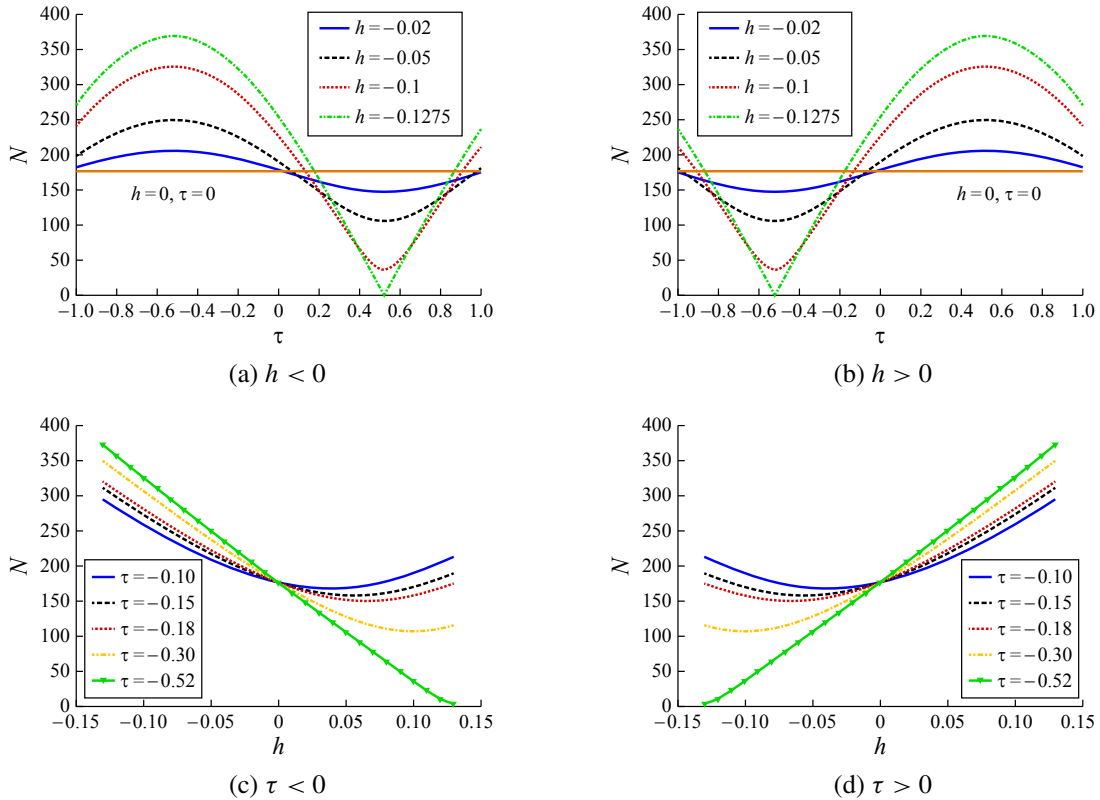


Figure 6. Relationships between the critical number of pedestrians and time delays and feedback adjustment factors.

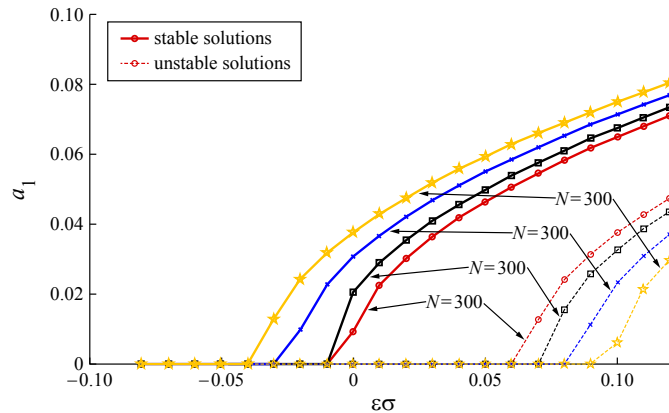


Figure 7. Amplitude-frequency response curves

- (1) The response amplitude has two different solutions, including the stable solution with a large value and the unstable solution with a small value. The curves of the two solutions are characterized by the rightward inclined shapes which are asymmetrically distributed around $\epsilon\sigma = 0$. This suggests

that bifurcations would occur at the point that is more than twice the first lateral frequency of bridge causing the divergent lateral vibration amplitudes.

- (2) When the number of pedestrians on the bridge decreases, the two solutions become closer to $\varepsilon\sigma = 0$ and the interval between them becomes smaller. This suggests that the number of pedestrians required to trigger the large lateral vibration decreases as the walking frequency arrives closer to the point that is twice the first lateral frequency of bridge.
- (3) The amplitude increases with the detuning parameter $\varepsilon\sigma$, suggesting that the amplitude would be larger as the walking frequency becomes greater than twice the bridge's first lateral frequency. Moreover, it is also observed that the curve tends to be more linear with the increase of $\varepsilon\sigma$, suggesting that the degree of nonlinearity would be weaker when the pedestrians' walking frequency becomes more than twice the bridge's first lateral frequency.

8. Conclusions

This study has used the Millennium Bridge as the background for an analysis of pedestrian-induced lateral vibration of a footbridge by considering the time delay and feedback adjustment that occur in the pedestrian-footbridge interaction. The main contributions of the present study can be summarized as follows:

- (1) The results of the qualitative analysis show that the time delay significantly affects the stability of the lateral vibration of footbridge. Moreover, the critical value of the time delay depends on the sign of the feedback adjustment factor.
- (2) The influences of time delay and feedback adjustment on response amplitude are significant. The time delay and feedback adjustment may cause a larger bridge amplitude than that without considering the time delay and feedback adjustment. The sign of feedback adjustment factor affects the distribution of bridge amplitude, while the time delay affects the trend of bridge amplitude.
- (3) The critical number of pedestrians depends on different combinations of time delay and feedback adjustment. In some cases, the time delay and feedback adjustment may cause a small value for the critical number of pedestrians, while in some other cases, the time delay and feedback adjustment may cause a large value for the critical number of pedestrians. By comparing with the experimental observation on the Millennium Bridge, the feedback adjustment factor and time delay corresponding to the large vibration of the Millennium Bridge may be the case of $\tau \in [-0.18, 0]$ and $h \in [0, 0.11]$, or the case of $\tau \in [0, 0.18]$ and $h \in [-0.11, 0]$.
- (4) When the walking frequency approaches the doubled first lateral frequency of bridge, a relatively small number of pedestrians is required to cause large lateral vibration.

References

- [Blekherman 2005] A. N. Blekherman, "Swaying of pedestrian bridges", *J. Bridge Eng.* **10**:2 (2005), 142–150.
- [Brownjohn et al. 2004a] J. M. W. Brownjohn, P. Fok, M. Roche, and P. Moyo, "Long span steel pedestrian bridge at Singapore Changi Airport, I: Prediction of vibration serviceability problems", *Struct. Eng.* **82**:16 (2004), 21–27.
- [Brownjohn et al. 2004b] J. M. W. Brownjohn, P. Fok, M. Roche, and P. Omenzetter, "Long span steel pedestrian bridge at Singapore Changi Airport, II: Crowd loading tests and vibration mitigation measures", *Struct. Eng.* **82**:16 (2004), 28–34.

- [Chopra 1981] A. K. Chopra, *Dynamics of structures: a primer*, Earthquake Eng. Res. Inst., Oakland, CA, 1981.
- [Dallard et al. 2001a] P. Dallard, A. J. Fitzpatrick, A. Flint, S. L. Bourva, A. Low, R. M. Ridsdill Smith, and M. Willford, “The London Millennium Footbridge”, *Struct. Eng.* **79**:22 (2001), 17–33.
- [Dallard et al. 2001b] P. Dallard, T. Fitzpatrick, A. Flint, A. Low, R. M. Ridsdill Smith, M. Willford, and M. Roche, “London Millennium Bridge: pedestrian-induced lateral vibration”, *J. Bridge Eng.* **6**:6 (2001), 412–417.
- [Fujino et al. 1993] Y. Fujino, B. M. Pacheco, S.-I. Nakamura, and P. Warnitchai, “Synchronization of human walking observed during lateral vibration of a congested pedestrian bridge”, *Earthq. Eng. Struct. Dyn.* **22**:9 (1993), 741–758.
- [Ingólfsson et al. 2012] E. T. Ingólfsson, C. T. Georgakis, and J. Jönsson, “Pedestrian-induced lateral vibrations of footbridges: a literature review”, *Eng. Struct.* **45** (2012), 21–52.
- [Liu and Xie 2013] L. Liu and W.-P. Xie, “Influence of time delay on the lateral vibration of footbridges induced by pedestrians”, *J. Civ. Eng. Manag.* **30**:1 (2013), 6–9, 15. In Chinese.
- [Nakamura 2004] S.-I. Nakamura, “Model for lateral excitation of footbridges by synchronous walking”, *J. Struct. Eng. (ASCE)* **130**:1 (2004), 32–37.
- [Newland 2004] D. E. Newland, “Pedestrian excitation of bridges”, *Proc. Inst. Mech. Eng. C, J. Mech. Eng. Sci.* **218**:5 (2004), 477–492.
- [Piccardo and Tubino 2008] G. Piccardo and F. Tubino, “Parametric resonance of flexible footbridges under crowd-induced lateral excitation”, *J. Sound Vib.* **311**:1-2 (2008), 353–371.
- [Qin 2013] J. W. Qin, *Human-structure interaction based on the bipedal walking model*, Ph.D. thesis, Beijing Jiaotong University, 2013. In Chinese.
- [Yuan 2006] X. Yuan, *Pedestrian-induced vibration characteristics of footbridges*, Ph.D. thesis, Tongji University, 2006. In Chinese.
- [Zhen et al. 2013] B. Zhen, W. Xie, and J. Xu, “Nonlinear analysis for the lateral vibration of footbridges induced by pedestrians”, *J. Bridge Eng.* **18**:2 (2013), 122–130.
- [Živanović et al. 2005] S. Živanović, A. Pavic, and P. Reynolds, “Vibration serviceability of footbridges under human-induced excitation: a literature review”, *J. Sound Vib.* **279**:1-2 (2005), 1–74.

Received 19 Jan 2017. Revised 25 May 2017. Accepted 30 May 2017.

JIA BUYU: ctjby@scut.edu.cn

School of Civil Engineering and Transportation, South China University of Technology, Guangzhou, China

CHEN ZHOU: cznew123@126.com

College of Transportation & Civil Engineering and Architecture, Foshan University, Foshan, China

YU XIAOLIN: xlyu1@scut.edu.cn

School of Civil Engineering and Transportation, South China University of Technology, Guangzhou, China

YAN QUANSHENG: cvqshyan@scut.edu.cn

School of Civil Engineering and Transportation, South China University of Technology, Guangzhou, China

JOURNAL OF MECHANICS OF MATERIALS AND STRUCTURES

msp.org/jomms

Founded by Charles R. Steele and Marie-Louise Steele

EDITORIAL BOARD

ADAIR R. AGUIAR	University of São Paulo at São Carlos, Brazil
KATIA BERTOLDI	Harvard University, USA
DAVIDE BIGONI	University of Trento, Italy
YIBIN FU	Keele University, UK
IWONA JASIUK	University of Illinois at Urbana-Champaign, USA
MITSUTOSHI KURODA	Yamagata University, Japan
C. W. LIM	City University of Hong Kong
THOMAS J. PENCE	Michigan State University, USA
GIANNI ROYER-CARFAGNI	Università degli studi di Parma, Italy
DAVID STEIGMANN	University of California at Berkeley, USA
PAUL STEINMANN	Friedrich-Alexander-Universität Erlangen-Nürnberg, Germany

ADVISORY BOARD

J. P. CARTER	University of Sydney, Australia
D. H. HODGES	Georgia Institute of Technology, USA
J. HUTCHINSON	Harvard University, USA
D. PAMPLONA	Universidade Católica do Rio de Janeiro, Brazil
M. B. RUBIN	Technion, Haifa, Israel

PRODUCTION production@msp.org

SILVIO LEVY Scientific Editor

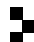
Cover photo: Wikimedia Commons

See msp.org/jomms for submission guidelines.

JoMMS (ISSN 1559-3959) at Mathematical Sciences Publishers, 798 Evans Hall #6840, c/o University of California, Berkeley, CA 94720-3840, is published in 10 issues a year. The subscription price for 2017 is US \$615/year for the electronic version, and \$775/year (+\$60, if shipping outside the US) for print and electronic. Subscriptions, requests for back issues, and changes of address should be sent to MSP.

JoMMS peer-review and production is managed by EditFLOW[®] from Mathematical Sciences Publishers.

PUBLISHED BY

 **mathematical sciences publishers**
nonprofit scientific publishing

<http://msp.org/>

© 2017 Mathematical Sciences Publishers

Journal of Mechanics of Materials and Structures

Volume 12, No. 5

December 2017

-
- Nonlinear impacting oscillations of pipe conveying pulsating fluid subjected to distributed motion constraints**
WANG YIKUN, NI QIAO, WANG LIN, LUO YANGYANG and YAN HAO 563
- Micro and macro crack sensing in TRC beam under cyclic loading** YISKA
GOLDFELD, TILL QUADFLIEG, STAV BEN-AAROSH and THOMAS GRIES 579
- Static analysis of nanobeams using Rayleigh–Ritz method**
LAXMI BEHERA and S. CHAKRAVERTY 603
- Analysis of pedestrian-induced lateral vibration of a footbridge that considers feedback adjustment and time delay**
JIA BUYU, CHEN ZHOU, YU XIAOLIN and YAN QUANSHENG 617
- Nearly exact and highly efficient elastic-plastic homogenization and/or direct numerical simulation of low-mass metallic systems with architected cellular microstructures** MARYAM TABATABAEI, DY LE and SATYA N. ATLURI 633
- Transient analysis of fracture initiation in a coupled thermoelastic solid**
LOUIS M. BROCK 667
- Geometrically nonlinear Cosserat elasticity in the plane: applications to chirality**
SEBASTIAN BAHAMONDE, CHRISTIAN G. BÖHMER and PATRIZIO NEFF 689
- Transient response of multilayered orthotropic strips with interfacial diffusion and sliding**
XU WANG and PETER SCHIAVONE 711



1559-3959(2017)12:5;1-0